

Theoretical Studies on Densification and Relaxation of Bubbly Glacier Ice

Andrey N. SALAMATIN¹ and Vladimir Ya. LIPENKOV²

気泡を含む氷床氷の圧密・緩和過程の理論的研究

Andrey N. SALAMATIN¹ • Vladimir Ya. LIPENKOV²

要旨: この解説は、筆者らがロシアにおいて1983年から1989年にかけて行った一連の研究のレビューである。均一な気泡を含む氷の圧密（あるいは膨張）過程の理論的検討を行う。極地氷床における密度の深度プロファイルおよび掘削後の体積膨張をシミュレーションするための数学的モデルを展開し、それを東南極ポストークにおける掘削コアに適用する。また、気泡から空気水和物結晶への遷移に対する簡単なモデルを提案する。

Abstract: This paper presents a brief review of the authors' earlier research on polar ice density modeling carried out and published (in the main) during 1983–1989 in Russia. A theoretical approach to macrocontinuum description of bubbly ice densification (expansion) on the basis of averaging asymptotic methods is considered. Mathematical models for the simulation of polar ice sheet density variations *versus* depth and for the prediction of deep ice core volume relaxation after its recovery are developed and tested on real situations at Vostok Station, East Antarctica. A simplified model of the equilibrium transformation of bubbles entrapped in ice into air hydrate crystals is proposed.

1. Introduction

The Russian deep drilling program in the central part of the Antarctic ice sheet at Vostok Station has been carried on since 1970 jointly by the Arctic and Antarctic Research Institute and St. Petersburg Mining Institute. It has resulted in obtaining unique experimental data concerning the dry polar firn and ice formation (transformation) processes as well as the ice core physical behavior at low temperature. Thus, theoretical research (LIPENKOV *et al.*, 1983, 1989; LIPENKOV and SALAMATIN, 1989; SALAMATIN *et al.*, 1985) was stimulated. The latter papers continued the studies by BADER (1965), GOW (1968, 1971), GOW and WILLIAMSON (1975) and LANGWAY (1958, 1967), performed for Site 2 in Greenland and Byrd Station in Antarctica. Parallel research on bubbly glacier ice core density and relaxation has been carried out by SHOJI and LANGWAY (1983) and by NAKAWO (1986).

It should be stated here that the snow-firn-ice transformation (densification)

¹ Kazan State University, 18, Lenin st., Kazan 420008, Russia.

² Arctic and Antarctic Research Institute, 38, Bering st., St. Petersburg 199226, Russia.

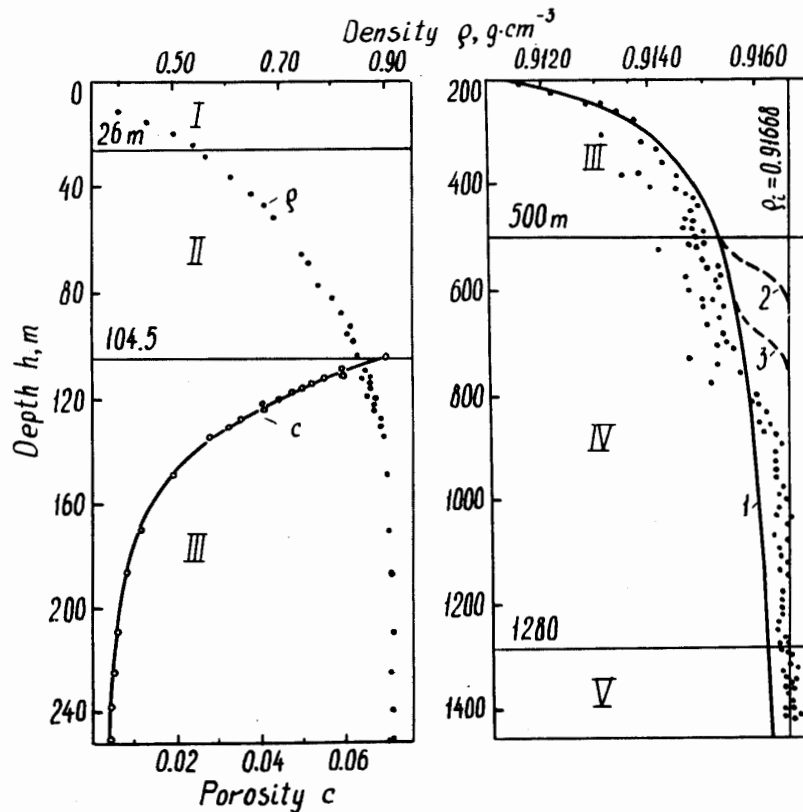


Fig. 1. Computed profiles and data of measurements of glacier ice density (dots) and porosity (circles) at Vostok Station. The curves are 1: with no regard to air-hydrate formation; 2: $p_d=3.3$ MPa; 3: $p_d=5.2$ MPa. I~V: The stages of ice densification.

process conventionally is represented by five stages. For Vostok Station they are described in LIPENKOV (1989) and SALAMATIN *et al.* (1985) and are shown in Fig. 1. Stage I is snow with a minimal volume concentration of closed pores $\sim 3-5 \cdot 10^{-3}$. Firn (consolidated snow), stage II, is marked by permanent growth of the impermeable pore space fraction *versus* depth. Bubbly glacier ice (stage III) begins at the pore close-off level of 104–105 m. Its bulk density increases as it sinks deeper because of the compression of discrete air inclusions. In stage IV the air-hydrate crystal formation from the initially entrapped bubbles becomes noticeable and primarily responsible for ice densification. Stage V is ice, which does not contain air.

The above-mentioned works by LIPENKOV and SALAMATIN mathematically model the bubbly ice densification in stage III as well as the reverse process of bubbly ice core relaxation after recovery. The principal objectives of the studies are (1) to account for the influence of the rheological properties of ice matrix containing air bubbles and (2) to separate the plain bulk densification (expansion) of ice due to the existing compression (decompression) of air inclusions from the air hydrate formation (dissociation) processes.

2. General Equations and Averaging Approach

Let us consider, following LIPENKOV *et al.* (1983) and SALAMATIN *et al.* (1985), a deformation of a cubical ice element K of dimensions $l \sim 1$ containing a large number N of identical gas bubbles of radius a (see Fig. 2). We also assume

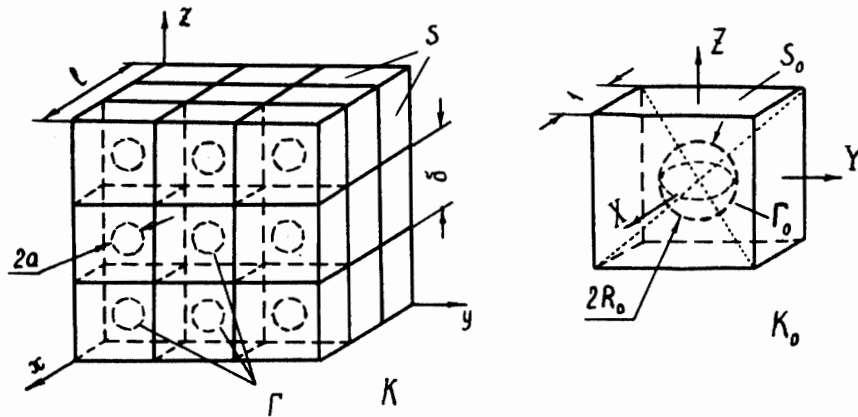


Fig. 2. The schematic periodic structure of bubbly ice.

that the bubbly ice has a periodic structure and consists of elementary cubic cells with edges of length $\delta = lN^{-1/3}$ parallel to Cartesian coordinate axes x, y, z which are the principal directions of strain. The bubbles are located in the cell centers. Obviously, their volume concentration (ice porosity) is $c = 4\pi a^3 / (3\delta^3)$.

Regarding the ice matrix as an incompressible non-Newtonian medium, one usually writes, after ASTARITA and MARRUCCI (1974), its rheological law in the form:

$$\sigma = -pI + 2\eta(4\dot{e}_{(2)})\dot{e}. \tag{1}$$

Here σ is the stress tensor, p —the pressure, I —the identity tensor, η is the rheological coefficient, which depends on the second invariant $\dot{e}_{(2)}$ of the strain rate tensor \dot{e} and temperature.

By definition

$$\dot{e} = 0.5(\nabla v + \nabla v^t), \quad \dot{e}_{(2)} = 0.5\dot{e} : \dot{e}, \tag{2}$$

where v is the velocity vector with components v_x, v_y, v_z , ∇ is the differential Hamilton operator, and the superscript “t” denotes transposition.

Stokes equations govern the creep non-inertia movement of the ice:

$$\nabla \cdot \sigma = 0, \quad \nabla \cdot v = 0. \tag{3}$$

At the gas-ice interface Γ we have

$$\sigma_{n|_r} = -np_b, \tag{4}$$

where n is the unit normal directed outside the ice matrix, and p_b is the bubble

pressure.

An arbitrary deformation of the glacier ice sample K can be defined by the macroscale axial strain rates q_x, q_y, q_z . In the case under consideration for the compression (decompression) processes in the bubbly ice the latter values are of the same order as the volume expansion rate $q = (q_x + q_y + q_z)/3$. To obtain the necessary relationship between q and the other parameters of the model (1)–(4) we introduce, after BAHVALOV and PANASENKO (1984) and BENSOUSSAN *et al.* (1978), an asymptotic averaging procedure, using the fact that the scale ratio $\varepsilon = \delta/l$ is small. Thus, the following expansions are valid:

$$\begin{aligned} v_x &= q_x x + \varepsilon u(X, Y, Z) + O(\varepsilon^2), & v_y &= q_y y + \varepsilon v(X, Y, Z) + O(\varepsilon^2), \\ v_z &= q_z z + \varepsilon w(X, Y, Z) + O(\varepsilon^2), & p &= p(X, Y, Z) + O(\varepsilon). \end{aligned} \quad (5)$$

Here u, v, w , and p are periodic functions of the “fast” coordinates $X = x/\varepsilon, Y = y/\varepsilon, Z = z/\varepsilon$ with the periodicity domain K_0 being the image of an elementary structural cell of the ice matrix (see Fig. 2).

Substituting eq. (5) into eqs. (1) and (2) for the components of the stress tensor σ we obtain:

$$\begin{aligned} \sigma_{xx} &= -p + 2\eta(4\dot{\varepsilon}_{(2)})\left(\frac{\partial u}{\partial X} + q_x\right), & \sigma_{xy} &= \eta(4\dot{\varepsilon}_{(2)})\left(\frac{\partial u}{\partial Y} + \frac{\partial v}{\partial X}\right), \dots, \\ \dot{\varepsilon}_{(2)} &= \frac{1}{4} \left[2\left(\frac{\partial u}{\partial X} + q_x\right)^2 + 2\left(\frac{\partial v}{\partial Y} + q_y\right)^2 + 2\left(\frac{\partial w}{\partial Z} + q_z\right)^2 + \left(\frac{\partial u}{\partial Y} + \frac{\partial v}{\partial X}\right)^2 \right. \\ &\quad \left. + \left(\frac{\partial u}{\partial Z} + \frac{\partial w}{\partial X}\right)^2 + \left(\frac{\partial v}{\partial Z} + \frac{\partial w}{\partial Y}\right)^2 \right]. \end{aligned} \quad (6)$$

Further, the x -axis projection of the momentum eq. (3) takes the form:

$$\begin{aligned} \frac{\partial p}{\partial X} &= 2 \frac{\partial}{\partial X} \left[\eta(4\dot{\varepsilon}_{(2)}) \left(\frac{\partial u}{\partial X} + q_x \right) \right] + \frac{\partial}{\partial Y} \left[\eta(4\dot{\varepsilon}_{(2)}) \left(\frac{\partial u}{\partial Y} + \frac{\partial v}{\partial X} \right) \right] \\ &\quad + \frac{\partial}{\partial Z} \left[\eta(4\dot{\varepsilon}_{(2)}) \left(\frac{\partial u}{\partial Z} + \frac{\partial w}{\partial X} \right) \right]. \end{aligned} \quad (7)$$

The other two, being similar, are omitted.

The equation of continuity is transformed in the following way

$$\frac{\partial u}{\partial X} + \frac{\partial v}{\partial Y} + \frac{\partial w}{\partial Z} + 3q = 0. \quad (8)$$

Finally, at the spherical air cavity surface Γ_0 located in the center of the cube K_0 , projecting the boundary eq. (4) onto the x -axis, one obtains:

$$\begin{aligned} \left[p_b - p + 2\eta(4\dot{\varepsilon}_{(2)}) \left(\frac{\partial u}{\partial X} + q_x \right) \right] n_x + \eta(4\dot{\varepsilon}_{(2)}) \left(\frac{\partial u}{\partial Y} + \frac{\partial v}{\partial X} \right) n_y \\ + \eta(4\dot{\varepsilon}_{(2)}) \left(\frac{\partial u}{\partial Z} + \frac{\partial w}{\partial X} \right) n_z = 0. \end{aligned} \quad (9)$$

It should be noted here that we actually deal with small values of the air volume concentration $c < 0.1$. In this case, as immediately follows from eq. (8), the

principal part of the microscale strain rates within the cell K_0 in eqs. (6), (7) originates from the volume deformation rate q and has the order q/c , being related to the difference between p_b and the ice macro pressure p_i by eq. (9). The deviatoric strains $q_x - q$, $q_y - q$, $q_z - q$, result in micro-strain rates of order q , and the corresponding parts of the stresses, being averaged over K_0 , give the deviator of the macro-scale stress tensor in the ice.

Hence, replacing q_x , q_y , q_z by q in eqs. (6), (7), (9), and in other analogous expressions, we come to the boundary value problem with respect to u , v , w , and p , that describes the compression (decompression) processes only. The resulting cell problem is analyzed by SALAMATIN *et al.* (1985) using Glen's rheological law:

$$\eta(\xi) = \mu^{1/\alpha} \xi^{(1-\alpha)/(2\alpha)}, \quad \alpha \geq 1,$$

in which α is the exponent (constant), and the factor μ depends on temperature. The approximate solution is found after replacing K_0 with the sphere of the equivalent volume. Thus, we directly obtain:

$$q = \frac{\beta c (p_b - p_i) |p_b - p_i|^{\alpha-1}}{3\mu(1-c^{1/\alpha})^\alpha}, \quad \beta = \alpha \left(\frac{\sqrt{3}}{2\alpha} \right)^{\alpha+1}. \quad (10)$$

On the other hand, the ice matrix is incompressible and the volume expansion rate q as well as variations of the air concentration c are entirely due to the change of bubble size (radius). Hence, the integration of eq. (8) over the ice volume within the cell K_0 yields the following relation

$$q = \frac{1}{3(1-c)} \frac{dc}{d\tau}, \quad (11)$$

where τ is the time.

Combining eqs. (10) and (11), we finally come to the principal result:

$$\frac{dc}{d\tau} = (\beta/\mu) (p_b - p_i) |p_b - p_i|^{\alpha-1} \frac{c(1-c)}{(1-c^{1/\alpha})^\alpha}. \quad (12)$$

The latter equation generalizes the findings by BADER (1965). It agrees the analogous relation obtained by WILKINSON and ASHBY (1975) on the basis of the cell model approach.

3. The Model of Densification of Bubbly Glacier Ice

The theoretical predictions and computations (LIPENKOV *et al.*, 1989; SALAMATIN *et al.*, 1985) of bubbly ice density and air volume concentration profiles in ice sheets are based on eq. (12). The density of glacier ice ρ can be, obviously, expressed in terms of the density of pure ice (ice matrix) ρ_i and the porosity c :

$$\rho = \rho_i(1-c), \quad (13)$$

with relative error not exceeding $5 \cdot 10^{-3}\%$.

Considering the bubble air to be an ideal gas and marking hereafter with the

subscript "o" the initial values of ice parameters at the depth and at the moment of the pore close-off, we obtain:

$$p_b = \gamma \frac{1-c}{c}, \quad \gamma = \frac{p_s \gamma_s T}{T_s}, \quad \gamma_s = \frac{c_o}{1-c_o} \frac{p_{bo} T_s}{p_s T_o}, \quad (14)$$

where $T = t + 273.15$ is the absolute temperature of the ice in K (t is the temperature in °C), the normal conditions are defined by $p_s = 0.1013$ MPa and $T_s = 273.15$ K.

It is relevant to emphasize the significance of the dimensionless complex γ_s as one of the main genetic characteristics of dry glacier ice (LIPENKOV, 1989).

Let us note, further, that the deviatoric part of the macro-stress tensor in the bubbly ice in a densification process is not zero. Therefore the ice macro pressure p_i is not exactly equal to the so-called load pressure. Nevertheless, preliminary estimations make it evident that, following SALAMATIN *et al.* (1985), with accuracy to several percent one can write

$$\partial p_i / \partial h = g \rho. \quad (15)$$

Here h is the depth, and g is the gravity acceleration.

To complete the model of bubbly ice densification we need the vertical downward (V) and, in the general case, longitudinal (U) velocities of the ice to determine the particle derivative in eq. (12): $dc/d\tau = \partial c/\partial \tau + V \partial c/\partial h + U \partial c/\partial s$ (s is the distance along the ice flow line under consideration). So, the general equations of glacier dynamics (SALAMATIN, 1992) must be used. At the same time it should be noticed that the densification processes take place within the near surface strata of ice sheets, where the longitudinal velocity is actually constant in the vertical direction. Taking this into account, one can transform, after LIPENKOV *et al.* (1989) and SALAMATIN (1992), the ice mass conservation equation into the following simplified form:

$$\frac{\partial V}{\partial h} = \frac{1}{1-c} \frac{dc}{d\tau} - \frac{1}{h_m} \left(1 + \frac{\nu}{\alpha + 1} \right) \left(A - V_m - \frac{\partial h_m}{\partial \tau} - \frac{Q}{h_m} \frac{\partial h_m}{\partial s} \right), \quad (16)$$

$$Q = \frac{1}{H} \int_0^s H(s) \left(A - V_m - \frac{\partial h_m}{\partial \tau} \right) ds,$$

where h_m is the glacier thickness in the equivalent of pure ice, A —the ice accumulation rate, V_m —the ice melting rate at the bed, H —the relative width of the ice flow tube with the current ice flow rate Q ; ν is an imitation parameter ($0 \leq \nu \leq 1$): $\nu = 0$ or 1, when there is no shear strain in the glacier body or no ice sliding in the basal layer respectively.

Equation (16) is accurate to order $\nu(h/h_m)^{\alpha+1}$. Terms of this order are negligible within at least the upper third of the ice sheet thickness, if, according to LLIBOUTRY (1979), the effective value of Glen's exponent α in non-isothermal conditions of ice shear flow is greater than 5. Moreover, it is easy to verify by straight estimation that the second term on the right-hand side of eq. (16) is one order less than the first term. Therefore, only its dominant part A/h_m can be retained in eq. (16) with the error not exceeding 3–5%.

To this end, combining eq. (12) and eqs. (13)–(16), we obtain after LIPENKOV *et al.* (1989) the following model of densification of dry bubbly ice in stage III:

$$\begin{aligned}\frac{dc}{d\tau} &= \frac{\beta}{\mu} \left(\gamma \frac{1-c}{c} - p_i \right) \left| \gamma \frac{1-c}{c} - p_i \right|^{\alpha-1} \frac{c(1-c)}{(1-c^{1/\alpha})^\alpha}, \\ \frac{\partial V}{\partial h} &= \frac{\beta}{\mu} \left(\gamma \frac{1-c}{c} - p_i \right) \left| \gamma \frac{1-c}{c} - p_i \right|^{\alpha-1} \frac{c}{(1-c^{1/\alpha})^\alpha} - \frac{A}{h_m}, \\ \partial p_i / \partial h &= g\rho_i(1-c).\end{aligned}\quad (17)$$

This is complete, if the surface conditions of the firn-ice formation vary negligibly up-stream along the flow line and $\partial c / \partial s \approx 0$.

Boundary values for c , V , and p_i must be determined at the close-off depth to identify the solution of the system (17). Integrating eq. (16) with respect to h , one can justify after LIPENKOV *et al.* (1989) the equality $V_o = A/(1-c_o)$ being accurate to 2–5%. Thus, additionally we have

$$c|_{h=h_o} = c_o, \quad V|_{h=h_o} = A/(1-c_o), \quad p_i|_{h=h_o} = p_{io}. \quad (18)$$

Further, in the upper part of the bubbly ice strata the second term on the right-hand side of eq. (16) is small and can be omitted. Consequently, in case of the stationary distribution of the air volume concentration c we obtain after SALAMATIN *et al.* (1985)

$$V = A/(1-c).$$

Correspondingly, eqs. (17) and (18) take the form:

$$\begin{aligned}\frac{dc}{dh} &= \phi \left(\gamma \frac{1-c}{c} - p_i \right) \left| \gamma \frac{1-c}{c} - p_i \right|^{\alpha-1} \frac{c(1-c)^2}{(1-c^{1/\alpha})^\alpha}, \\ dp_i/dh &= g\rho_i(1-c); \\ c|_{h=h_o} &= c_o, \quad p_i|_{h=h_o} = p_{io},\end{aligned}\quad (19)$$

where $\phi = \beta/\mu A$.

The latter model had been used by SALAMATIN *et al.* (1985) to simulate the ice density (air concentration) profiles in five bore-holes drilled in the Antarctic ice sheet (at Vostok, Vostok-I, Pionerskaya, and Byrd Stations) and in Greenland (at Site 2).

All the computations are based on the data from deep ice core studies by LIPENKOV (1989), SMIRNOV (1983), GOW (1968), and LANGWAY (1958, 1967). The chosen bore-holes represent a wide range of dry ice formation conditions: $h_o \sim 60$ –105 m, $A \sim 2.4$ –42.4 cm/y, $c_o \sim 0.07$ –0.104, $p_{bo} \sim 0.063$ –0.081 MPa, $p_{io} \sim 0.5$ –0.74 MPa, $T_o \sim 218$ –248 K, $\gamma_s \sim 0.058$ –0.103. For each of the five cases the model parameters α and μ (*i.e.* ϕ) are determined, and the values of c_o , p_{bo} are also verified through an inverse procedure on the assumption that $T = T_o$ and $\gamma = p_s \gamma_s$. The best fits between the observed and computed air concentration profiles to depth of 250–270 m are found by minimizing the mean square deviations S in accordance with the

gradient method of steepest descent.

The minimal values of $S \sim 10^{-3}$ for Vostok and $\sim 2-5 \cdot 10^{-3}$ for the other sites correspond to Glen's exponent $\alpha \approx 3.8 \pm 0.6$ and are practically insensitive to variations of α within these limits. As a result, for $\alpha = 3.8$ the rheological coefficient μ is deduced as a function of temperature

$$\mu(t) = \mu_* \exp[-kt/(t+273)], \quad k = 36, \quad \mu_* = 3 \cdot 10^{-3} \text{ MPa}^\alpha \cdot \text{y}. \quad (20)$$

The apparent activation energy in the Arrhenius factor is 82 kJ/mole (19 kcal/mole). The best fit profile of the air volume concentration for Vostok Station ($A = 2.38$ cm/y, $\rho_i = 923$ kg/m³, $c_o = 0.07$, $p_{bo} = 0.063$ MPa, $p_{io} = 0.742$ MPa, $t_o = -55^\circ\text{C}$, $\gamma_s = 0.0586$) is depicted in Fig. 1a by a solid line. Dots and empty circles are the data from measurements.

Finally, following SALAMATIN *et al.* (1985), for relatively large h , as $c \rightarrow 0$ and $p_b \rightarrow p_i$, from eq. (19) we obtain:

$$(p_i - p_b)^\alpha = \frac{g\rho_i}{\gamma\phi} \frac{c(1-c^{1/\alpha})^\alpha}{1-c} + o(c^2), \quad \frac{dc}{dh} = -\frac{g\rho_i}{\gamma} c^2(1-c) + o(c^3).$$

Hence, asymptotically c does not depend on the ice rheological properties and, if $c_1 = c(h_1)$, then:

$$h - h_1 \approx \frac{\gamma}{g\rho_i} \left(\frac{1}{c} - \frac{1}{c_1} + \ln \frac{c_1}{c} \right), \quad h > h_1 \gg h_o. \quad (21)$$

This relationship at $h_1 = 209$ m and $c_1 = 0.0057$ for Vostok Station gives the density profile shown by a solid line in Fig. 1b.

A noticeable discrepancy between the curve and the ice core density measurements within the interval of 300–600 m indicates that this ice stratum had formed under different climatic conditions and has different values of the genetic characteristic γ_s .

The general model (17), (18) and its sensitivity to variations of the boundary ice parameters at the pore close-off level had been investigated in (LIPENKOV *et al.*, 1989).

4. Ice Core Relaxation After Its Recovery

The number and the volume of initially entrapped air inclusions decrease abruptly in stage IV of ice densification due to transformation of air into air hydrate crystals (see, for example, Fig. 1b, the depth interval 650–850 m at Vostok). Correspondingly, relaxation of ice cores after their recovery actually results from two different processes: (1) expansion of the primary bubbles under decompression and (2) dissociation of hydrates and formation of secondary inclusions of air. The first studies of this phenomenon in the deep ice core from Vostok are presented by LIPENKOV (1989), LIPENKOV and SALAMATIN (1989), and SALAMATIN *et al.* (1985).

Let us consider, following LIPENKOV and SALAMATIN (1989), a mathematical

model of the bulk expansion of the ice samples attributed to decompression of primary air bubbles after removal of the ice from high confining pressures.

From eqs. (12) and (14), we obtain:

$$\frac{dc}{d\tau} = \frac{\beta}{\mu} \left[\gamma \frac{1-c}{c} - p_i \right]^\alpha \frac{c(1-c)}{(1-c^{1/\alpha})^\alpha}, \quad c|_{\tau=0} = c_* \quad (22)$$

Here p_i is the external (atmospheric) pressure, τ —the time of ice sample storage, and c_* —the initial (*in situ*) porosity of ice.

As a rule, $p_b = \gamma(1-c)/c \gg p_i$ in eq. (22), which can be rewritten in a simplified form:

$$\int_{c_*}^c \frac{\zeta^{\alpha-1} (1-\zeta^{1/\alpha})^\alpha}{(1-\zeta)^{\alpha+1}} d\zeta = \frac{\beta\gamma^\alpha}{\mu} \tau.$$

For small c with relative error not exceeding $0.5(\alpha+1)(\alpha+2)c^2$ we have:

$$\int_{c_*}^c \zeta^{\alpha-1} (1-\zeta^{1/\alpha})^\alpha d\zeta + (\alpha+1) \int_{c_*}^c \zeta^{\alpha-1} (1-\zeta^{1/\alpha})^\alpha d\zeta = \frac{\beta\gamma^\alpha}{\mu} \tau.$$

The integrals on the left-hand side of this equality can be evaluated via hypergeometric series. Thus, we finally obtain

$$c^\alpha f(c, \alpha) = \alpha\beta\gamma^\alpha \tau / \mu + c_*^\alpha f(c_*, \alpha), \quad (23)$$

where

$$\begin{aligned} f(c, \alpha) = & 1 - \frac{\alpha^3}{\alpha^2+1} c^{1/\alpha} + \frac{\alpha^3(\alpha-1)}{2(\alpha^2+2)} c^{2/\alpha} - \frac{\alpha^3(\alpha-1)(\alpha-2)}{6(\alpha^2+3)} c^{3/\alpha} \\ & + \frac{\alpha^3(\alpha-1)(\alpha-2)(\alpha-3)}{24(\alpha^2+4)} c^{4/\alpha} \dots \\ & + \alpha c \left[1 - \frac{\alpha^2(\alpha+1)}{\alpha^2+\alpha+1} c^{1/\alpha} + \frac{\alpha^2(\alpha^2-1)}{2(\alpha^2+\alpha+2)} c^{2/\alpha} \dots \right]. \end{aligned}$$

The deduced approximate solution had been applied by LIPENKOV and SALAMATIN (1989) to analysis and interpretation of the relaxation processes in the Vostok ice core. A special collection of samples had been prepared, kept and observed for 200–300 days in the Glaciological Laboratory at Vostok Station by LIPENKOV (1989).

It follows from eq. (23) that the expansion of primary air bubbles at a fixed temperature is controlled by two independent parameters: c_* , α and also by the complex parameter: $\alpha\beta\gamma^\alpha/\mu$. Hence, the rheological properties of the ice must be determined to distinguish the influence of ice genesis characteristic γ . In particular, according to the findings by SALAMATIN *et al.* (1985), the values: $\alpha = 3.8$ and $\mu = 1.3 \cdot 10^{-2} \text{ MPa}^\alpha \cdot \text{y}$ (see eq. (20) in the previous section) are used in computations of porosity increase for samples numbered from 1 to 6 from the depths of 313, 383, 519, 622, 880, and 1030 m (respectively) stored at the temperature $t = -11^\circ \text{C}$.

The first pair contained only entrapped air in the gaseous phase. Secondary gas

inclusions appeared in the next two samples 5 and 3.5 months after their recovery. Air hydrate dissociation in the Vostok ice recovered from depths below 800 m begun within several days.

To eliminate the effect of ice core fracturing during drilling the *in-situ* ice porosity c_* and the genetic characteristic γ for the four upper depth levels are determined by minimizing the mean square deviation between computed and measured air volume concentrations in the samples 1–4 over the storage periods before the beginning air hydrate dissociation: $c_* = 4.15, 2.78, 1.05, 0.95 \cdot 10^{-3}$, $\gamma = 5.2, 6.1, 4.8, 4.3 \cdot 10^{-3}$ MPa, respectively. A comparison of the experimental data on the ice core porosity changes and the theoretical predictions of primary air bubbles expansion for each of the six samples is given in Fig. 3. The contribution of the clathrate decomposition to the deep ice core relaxation is seen and can be quantitatively estimated.

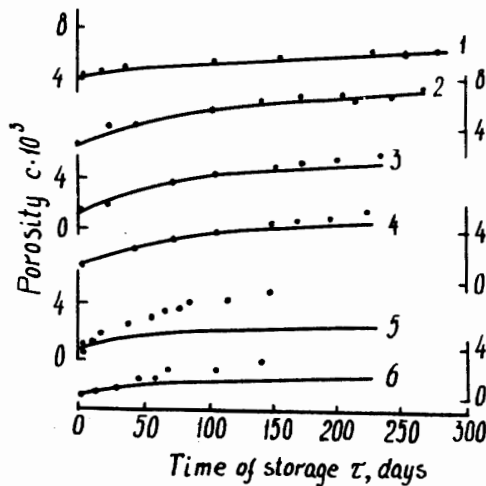


Fig. 3. Computed (solid lines) and measured (dots) change of the ice sample porosity versus time at the temperature of -11°C after the ice core recovery. The depths are 1: 313 m; 2: 383 m; 3: 519 m; 4: 622 m; 5: 880 m; 6: 1030 m.

Another peculiarity of the process studied should be mentioned. The *in-situ* bubble pressure p_{b*} is easily evaluated in accordance with eq. (14), when c_* and γ are known. For samples 3 and 4 containing air hydrate crystals it appears to be 3.6–3.7 MPa, which is close to the dissociation pressure $p_d \sim 3.3$ –3.4 MPa in the corresponding interval of 500–650 m at Vostok Station.

5. Remarks on the Model of Equilibrium Formation of Air Hydrates in Glacier Ice

The investigations of bubbly ice densification and relaxation processes at Vostok described above suggest that the air bubbles may transform into air hydrate crystals at pressures not significantly exceeding the equilibrium dissociation pressure p_d . Hence, in eq. (12) for stage IV, $p_b \approx p_d$ instead of the former relation (14) used for stage III. Consequently, the model (17) of bubbly ice densification can be generalized by assuming, after LIPENKOV (1989):

$$\gamma = \begin{cases} p_s \gamma_s T / T_s, & p_d c / (1 - c) > p_s \gamma_s T / T_s; \\ p_d c / (1 - c), & p_d c / (1 - c) < p_s \gamma_s T / T_s. \end{cases} \quad (24)$$

The resulting system of eqs. (17), (18) and (24) is solved numerically by LIPENKOV *et al.* (1989). The computed ice density profiles for Vostok at $p_d = 3.3$ and 5.2 MPa are shown in Fig. 1b by dashed lines. In spite of the evident qualitative similarity to experimental data, the theoretical predictions for air-ice equilibrium conditions yield too high rates of hydrate formation. Thus, an improved model of glacier ice densification in stage IV must be developed for quantitative analysis of the latter process.

6. Conclusion

The theoretical survey undertaken proves the averaging asymptotic methods to be a useful instrument in mathematical modeling of densification and relaxation processes in ice sheets and ice cores. The rheological properties of the glacier ice are inferred from air volume concentration (ice porosity) profiles in five bore-holes drilled in Antarctica and Greenland. These results do not contradict the known experimental laboratory data (BUDD, 1969) and agree with the corresponding estimations deduced for different ranges of stresses by modeling the bore-hole closure in the ice massif at Vostok Station (SALAMATIN *et al.*, 1981) and the East Antarctic ice sheet flow (SALAMATIN *et al.*, 1982). The developed mathematical models quantitatively describe the behavior of the bubbly glacier ice under compression or decompression in stage III without formation or dissociation of air hydrate crystals. At the same time they reveal the contribution of the latter processes to the ice densification or ice core relaxation in stage IV. The construction of mathematical models taking into account the transformation of air bubbles into air hydrates in the ice is of primary interest.

Acknowledgments

The authors are grateful to Prof. T. HONDOH (Hokkaido University, Sapporo) and Prof. Y. FUJII (National Institute of Polar Research, Tokyo) for interest in their research for the suggestion to write this paper for the Antarctic Record.

References

- ASTARITA, G. and MARRUCCI, G. (1974): Principals of non-Newtonian fluid mechanics. McGRAW-HILL.
- BADER, H. (1965): Theory of densification of dry, bubbly glacier ice. CRREL Res. Rep., **141**, 1–16.
- BAHVALOV, N. S. and PANASENKO, G. P. (1984): Osredneniye protsessov v periodicheskikh sredah (Averaging of processes in periodic mediums). Moscow, Nauka.
- BENSOUSSAN, A., LIONS, J.-L. and PAPANICOLAOU, G. (1978): Asymptotic analysis for periodic structures. Amsterdam, North-Holland.
- BUDD, W. F. (1969): The dynamics of ice masses. ANARE Sci. Rep., Ser. A (IV) Glaciology, **108**, 216 p.
- GOW, A. J. (1968): Bubbles and bubble pressures in Antarctic glacier ice. CRREL Res. Rep., **249**, 1–16.

- GOW, A. J. (1971): Relaxation of ice deep drill cores from Antarctica. *J. Geophys. Res.*, **76**, 2533–2541.
- GOW, A. J. and WILLIAMSON, T. (1975): Gas inclusions in the Antarctic ice sheet and their glaciological significance. *J. Geophys. Res.*, **80**, 5101–5108.
- LANGWAY, C. C., Jr. (1958): Bubble pressure in Greenland glacier ice. *Physics of the Movement of Ice*. Gentbrugge, Association Internationale d'Hydrologie Scientifique, 336–350 (IAHS Publ. 47).
- LANGWAY, C. C., Jr. (1967): Stratigraphic analysis of a deep ice core from Greenland. *CRREL Res. Rep.*, **77**, 1–130.
- LIPENKOV, V. Ya. (1989): Obrazovaniye i razlozheniye gidratov vozduha v lednikovom l'du (Formation and dissociation of air hydrates in glacier ice). *Mater. Glyatsiol. Issled. (Data of Glaciological Studies)*, **65**, 58–64.
- LIPENKOV, V. Ya. and SALAMATIN, A. N. (1989): Relaksatsionnoye rasshireniye ledyanogo kerna iz burovoy skvazhini na st. Vostok (Volume relaxation of the ice core from the bore hole at Vostok Station). *The Antarctic (The Committee Reports)*, **28**, 59–72.
- LIPENKOV, V. Ya., SALAMATIN, A. N. and SMIRNOV, K. E. (1983): O reologicheskikh svoystvah i deformatsii l'da s puzirkami gasa (On rheological properties and deformation of ice with gas bubbles). *Tez. dokl. na II Vsesoyuz. konf. po mehan. i fiz. l'da (Abstracts of the reports at the II All-Union Conf. on mech. and phys. of ice)*, Moscow, Nov., 15–18, 1983, 51–52.
- LIPENKOV, V. Ya., SALAMATIN, A. N. and GRIGORIEVA, Yu. A. (1989): Matematicheskaya model i chislennoye issledovaniye protsessa uplotneniya lednikovogo l'da (Mathematical model and numerical studies of glacier ice densification process). *Mater. Glyatsiol. Issled. (Data of Glaciological Studies)*, **65**, 49–58.
- LLIBOUTRY, L. (1979): A critical review of analytical approximate solutions for steady state velocities and temperatures in cold ice-sheets. *Z. Gletscherkd. Glazialgeol.*, **15**(2), 135–148.
- NAKAWO, M. (1986): Volume expansion of a 413.5 m-Mizuho core after its recovery. *Mem. Natl. Inst. Polar Res., Spec. Issue*, **45**, 78–85.
- SALAMATIN, A. N. (1992): Ice sheet modeling taking account of glacier ice compressibility. *Glaciers-Ocean-Atmosphere Interactions*, ed. by V. M. KOTLYAKOV *et al.* Wallingford, IAHS Press, 183–192 (IAHS Publ. 208).
- SALAMATIN, A. N., CHISTYAKOV, V. K., DMITRIEV, D. N. and PASHKEVICH, V. M. (1981): Teoreticheskii analiz i eksperimental'noye issledovaniye deformatsii stenok stvola skvazhini v ledovom massivye (Theoretical analysis and experimental investigation of the well wall deformation in the ice massif). *The Antarctic (The Committee Reports)*, **20**, 135–143.
- SALAMATIN, A. N., LIPENKOV, V. Ya., SMIRNOV, K. E. and ZHILOVA, Yu. V. (1985): Plotnost' lednikovogo l'da i ego reologicheskkiye svostva (Density of glacial ice and its rheological properties). *Antarktika (The Antarctic)*, **24**, 94–106.
- SALAMATIN, A. N., SMIRNOV, K. E. and SHEREMET'YEV, A. N. (1982): Primeneniye matematicheskoy modeli statsionarnogo lednika k raschyotu termogidrodinamicheskikh harakteristik lednikovogo pokrova Antarktidi v rayonye marshruta ot Mirnogo k kupolu B (Application of the mathematical model of a stationary glacier to the computations of the thermohydrodynamic characteristics of the Antarctic ice sheet in the vicinity of Mirniy—Dome B traverse). *Mater. Glyatsiol. Issled. (Data of Glaciological Studies)*, **44**, 39–49.
- SHOJI, H. and LANGWAY, C. C., Jr. (1983): Volume relaxation of air inclusions in a fresh ice core. *J. Phys. Chem.*, **87**, 4111–4114.
- SMIRNOV, K. E. (1983): Issledovaniye razreza lednikovogo pokrova v rayonye stantsii Pionerskoy (Vostochnaya Antarktida) (Studies of the cross-section of the ice sheet in the vicinities of Pionerskaya Station (East Antarctica)). *Mater. Glyatsiol. Issled. (Data of Glaciological Studies)*, **46**, 128–132.
- WILKINSON, D. S. and ASHBY, M. F. (1975): Pressure sintering by power law creep. *Acta Metall.*, **23**, 1277–1285.

(Received June 30, 1993)